

Direct monitoring of biochemical processes using micro-structured heat power detectors

J. Lerchner*, A. Wolf, R. Hüttl, G. Wolf

TU Bergakademie Freiberg, Institute of Physical Chemistry, Leipziger Street 29, D-09596 Freiberg, Germany

Abstract

An improved flow-through chip calorimeter useful for liquid samples is presented. The heat power detection limit could be decreased to a level of 180 nW. Main features of the new micro-sized calorimeter are a differential chip arrangement, a small sized thermostat with a precision in the micro-kelvin range and the application of micro-pumps for liquid flow control. The improved heat power resolution enables the monitoring of biochemical processes under relevant conditions. As applications have shown a pulsed fluid injection can increase the degree of mixing. For the determination of the degree of mixing a new method was developed.

© 2003 Elsevier B.V. All rights reserved.

Keywords: Calorimetry; Flow-through chip calorimeter; Enzymes; Micro-kelvin thermostat; Degree of mixing

1. Introduction

Because of the universal nature of the heat power production of chemical reactions the measurement of the evolved heat opens an elegant way to study directly elementary processes in biochemistry. In fact, no sophisticated cascades of reaction steps are necessary to generate signals which are related to the primary reaction under investigation. On the other hand, a calorimetric equipment which is necessary to obtain reasonable information from such kind of processes is rather ambitious. Usually, the amount of the available sample is strongly limited. Beyond that, the low concentration of the active species, as for example peptides, decreases the heat power density. In Table 1 relevant data of some biochemical processes are summarised which illustrate the demands on the detection limits of the heat power measurement. The first three processes are enzyme catalysed reactions followed by two aerobic and one anaerobic degradations of substrates by living micro-organisms. The last row contains representative data of antigen–antibody reactions. The degree of conversion means the relationship from the amount of converted substrate to the amount of the injected ones. It depends on the activity of the enzymes and the micro-organism as well as on the mixing efficiency of the measuring device. In all cases a continuous flow-through operation mode is assumed. For the given concentrations and assuming representative operation

parameters of a micro-sized flow-through calorimeter the heat power dissipation was estimated. It is to be recognised clearly that a heat power resolution below the micro-watt range is desirable if relevant applications should be possible.

Micro-sized flow-through calorimeters are usually developed on the basis of thermopile silicon chips [1,2]. Since several years we are studying the possibilities of application of micro-structured devices in calorimetry. On the basis of micro-machined silicon chips with integrated thermopiles as temperature sensing elements we have constructed so-called *integrated circuit* (IC) calorimeters (also named as chip calorimeters) useful for various purposes [3–5]. Due to the applied semiconductor technology the heat power sensitivity of the used thermopile chips [6] exceeds the corresponding data of conventional calorimeters by many degrees. That is at all the most substantial precondition for the construction of miniaturised calorimeters with reasonable capabilities. The main reasons for the high demands on the sensitivity are the reduced volume of the reaction chamber and the limitation of the degree of mixing which decreases the amount of the overall available heat power.

For the study of liquid samples the application of chip calorimeters is not ideal. The main advantage of chip calorimeters are their low time constants which are in the range of a few milliseconds. This feature can be successfully used for the investigation of thin coatings directly deposited onto the surface of the chip membrane, e.g. for the determination of heats of absorption [7,8], heat capacities at high frequencies [9] and for the measurement of heats of melting of small metal clusters [10]. However,

* Corresponding author. Tel.: +49-37-3139-2125;

fax: +49-37-3139-3588.

E-mail address: johannes.lerchner@chemie.tu-freiberg.de (J. Lerchner).

Table 1

Heat power generation of some biochemical processes (estimated assuming a volume flow rate of $v = 20 \mu\text{l min}^{-1}$, a chamber volume of $V = 20 \mu\text{l}$ and an enzyme activity of 200 U ml^{-1})

Process	ΔH (kJ mol ⁻¹)	Concentration, c (mmol l ⁻¹)	Degree of conversion, D	Heat power (μW)
Glucose (GOD/catalase)	225	0.1	0.7	7
Urea (urease)	61	0.1	0.5	1
Sucrose (invertase)	15	0.1	0.5	0.25
Phenol (Rhodococcus)	200	0.24	0.65	10
Glucose (Saccharomyces)	2870	0.24	0.1	24
Anaerobe degradation	100	1	0.003	0.2
Antibody–antigen reaction	70	0.01	0.9	0.1

liquid samples need to be covered by a reaction chamber in order to avoid evaporation effects. This increases the time constant remarkably. Evaporation effects in free standing samples caused by vapour pressure changes limit the resolution of the heat measurement to approximately $50 \mu\text{J}$ [3]. The time constants of flow-through chip-devices for liquids are in the range of some seconds. As a consequence, the influence of external temperature perturbations is increased and the experimental effort for temperature control has to be extended. Further the reduced mixing efficiency due to the laminar flow conditions has to be taken into account.

Nevertheless the application of micro-sized calorimeters is attractive: the investigation of very small samples is possible, the operation is much faster in comparison with conventional calorimeters and micro-sized calorimeters can be applied as analytical tools. Therefore, we have made some attempts in the last time to improve the heat power resolution of flow-through chip calorimeters for liquid samples. In this paper, we aim to describe new experimental features of a silicon chip-based flow-through calorimeter:

- a differential chip calorimetric arrangement with high performance to suppress remaining temperature perturbations;
- the design of a miniaturised calorimetric module with micro-kelvin-temperature control;
- the adaptation of micro-sized devices for fluid flow control.

2. Experimental

2.1. Differential chip arrangement

The heat power detection limit of flow-through chip calorimeters is essentially determined by the signal voltage noise, the stability of the reference temperature of the thermopile and of the fluid flows, respectively. Further pressure pulses induced by fluid pumps, gas bubbles and electronic effects due to the change of the ionic strength of the liquid can generate noise effects. Unfortunately, solid-state integrated thermopiles have a rather high electrical resistance (i.e. $50 \text{ k}\Omega$ for the LCM 2425 chip in comparison with 5Ω for a conventional thermopile module). Thus Johnson noise

as well as amplifier noise restrict the heat power detection limit to approximately 50 nW assuming a sensitivity of 2 V W^{-1} and a band width of 1 Hz . As a consequence, the performance of the temperature control should limit temperature induced disturbances in the heat power measurement to a range of lower than 100 nW .

Fig. 1 depicts the scheme of an arrangement of two thermally coupled thermopile chips NCM-9924 (improved version of the chip LCM 2425 manufactured by Xensor Integration, Netherlands [6]). Aim of the coupling is the reduction of signal noise caused by temperature perturbations in the surroundings. The upper chip (measuring chip) is joined with a flow-through reaction chamber (PMMA). The inlet flows enter the reaction chamber at the inlet ports (see Fig. 3). A detailed description of the reaction chamber is given in [11]. At slow changes the influence of external temperature perturbations on the signal depends only on the heat capacity of the sample [12]. A reaction chamber of a volume of $20 \mu\text{l}$ filled with aqueous sample corresponds to a heat capacity of 100 mJ K^{-1} . In this case stochastic temperature perturbations of $200 \mu\text{K}$ (standard deviation) with a band width of 1 mHz generate a heat power noise of approximately 100 nW . One way to reduce this kind of noise is to apply the classical principle of a differential calorimeter. In the described device two chips are joined face-to-face by a 2 mm thick aluminium frame which is positioned near the reference junctions of both thermopiles. In order to prevent direct thermal coupling of the hot junctions of the thermopiles thermal shielding is necessary. The reference chip is loaded with an inert sample (graphite cylinder of 4 mm diameter and 2 mm height). Because it is practically impossible

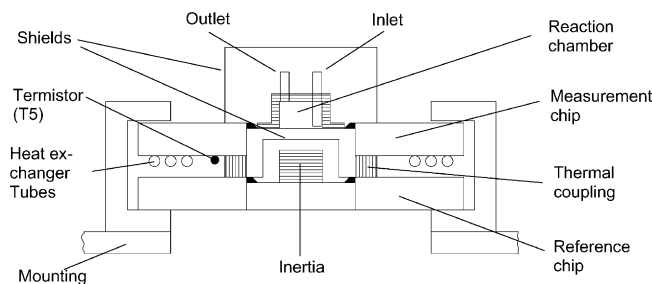


Fig. 1. Scheme of the differential chip arrangement.

to establish equal thermal conditions for both chips the thermopile signal of the reference chip cannot be used for corrections without previous processing (see below).

2.2. Micro-kelvin thermostat

Despite of the application of correction procedures as described above a precise temperature control is necessary. One has to be aware that temperature fluctuations of $50 \mu\text{K}$ of an aqueous fluid flow of $20 \mu\text{l min}^{-1}$ produce 70 nW heat power noise. Therefore, some effort was made in order to design a precise thermostat with a size adequate to a chip calorimeter.

The developed two-stage thermostat consists of two nested U-shaped frames (see Figs. 2 and 3). The chip arrangement is mounted inside the inner frame. The outer and inner frames are made of 4 mm thick aluminium and 5 mm thick copper, respectively. At the outer side of the walls four foil heaters are attached. In order to enable fast response the temperature sensors T1–T2 ($10 \text{ k}\Omega$ thermistors) are placed inside the walls near the foil heaters. Only one sensor of every frame is used as regulating sensor. The symmetry of the design assures a sufficiently constant temperature in both walls of the frames. For temperature control digital implemented PID controllers with optimised parameters were used. The control temperatures for the outer and inner frame were set to 25 and 25.3°C , respectively. The reference

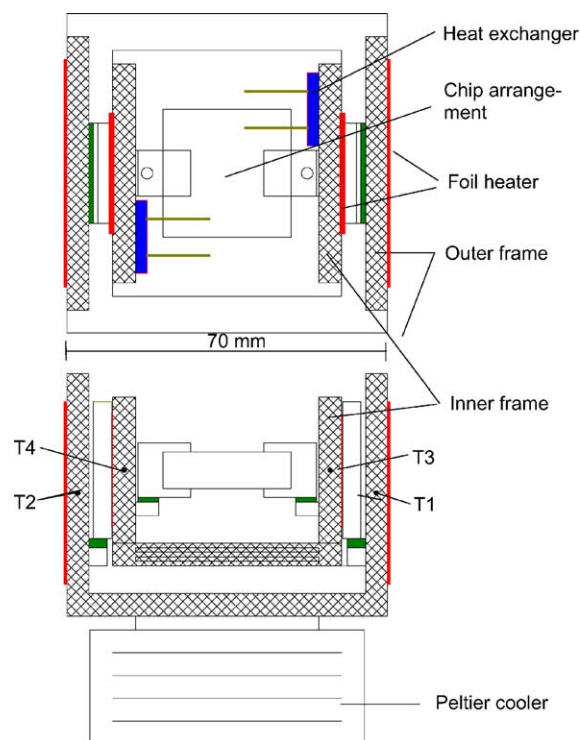


Fig. 2. Scheme of the micro-kelvin thermostat (T1, T3—regulating and measuring thermistors; T2, T4—measuring thermistors).

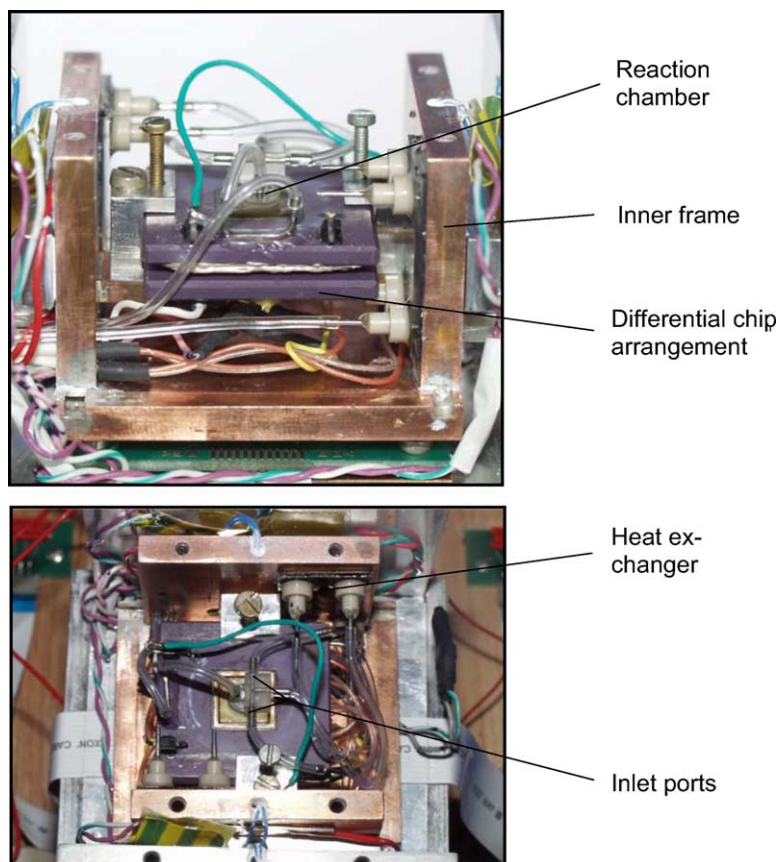


Fig. 3. Photograph of the inner frame of the thermostat with the installed chip arrangement.

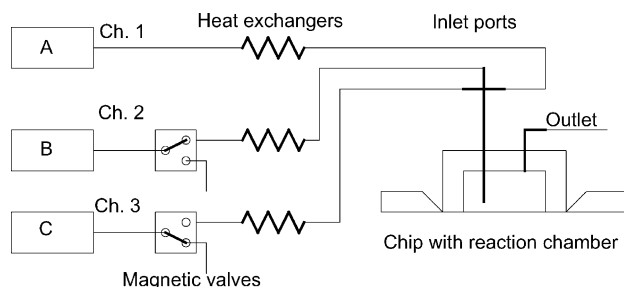


Fig. 4. Scheme of the fluid flow system.

temperature of the upper chip is monitored by an additional sensor (T5). A peltier module serves as constant power heat sink. Three micro-machined silicon-glass heat-exchanger (IPHT Jena, Germany) for temperature equilibration of the input fluid flows are attached at the walls of the inner frame. The coils which are mounted below the upper chip (see Fig. 1) are used for final temperature equilibration of the flows. Two U-shaped lids of the same size and material as the frames (not shown in the figures) make up two closed chambers.

2.3. Fluid control

A simplified scheme of the fluid flow system is shown in Fig. 4. Through channel 1 component A is permanently injected. Two other flows are controlled by magnetic valves (LEE Company, USA) in order to initiate the reactions by switching between components B and C. The flow system is equipped with a syringe pump (SP 200 World Precision, USA). Volume flow rates in the range between 0 and $30 \mu\text{l min}^{-1}$ were applied. In order to test the suitability of micro-pumps the syringe of channel 2 was replaced by different types of micro-pumps in some experiments. Up to now we successfully tested the micro-pumps XXS500 (thinXXS, Germany) and LPV (LEE Company, USA). Because the investigations are still in progress summarised results of the tests will be presented in a future paper. The control unit of the pumps enables different modes of operation. In the continuous flow mode the pumps are activated permanently. In the impulse injection mode separate volume increments can be injected. If the volume increments are larger than the volume of the reaction chamber it is better to term it as stopped-flow mode. For example, the stopped-flow mode can be used to determine the degree of conversion. In the impulse injection mode the flow rate dependence of the sensitivity is not relevant. Further the degree of conversion has not to be taken into account. On the other hand pressure effects must be corrected.

2.4. Test reactions

In order to demonstrate the performance of the chip calorimeter the results of two test reactions are presented.

As example for a fast reaction the protonisation of TRIS (tetrahydroxy-methylaminomethane) by hydrochloric acid was applied. In the continuous flow mode TRIS solution is continuously injected, whereas the variable flows were switched between hydrochloric acid (B, channel 2) and distilled water (C, channel 3). In the flow injection mode the calorimeter inlet ports are permanently connected with channels 1 and 2. The second reaction is a model system for the intended biochemical application of the chip calorimeter. We have chosen the enzyme catalysed oxidation of β -D-glucose. To improve the sensitivity of the reaction the enzyme glucose oxidase (EC 1.1.3.4) was coupled with the enzyme catalase (EC 1.11.1.6). The activity of the used enzyme solution was 250 and 280 U ml^{-1} for glucose oxidase and catalase, respectively. Glucose (A) and the enzymes (B) were solved in 0.1 mol l^{-1} phosphate buffer of $\text{pH} = 6.9$. Pure buffer solution was used as component C.

3. Results and discussion

3.1. Verification of the correction procedure

As mentioned above time constants and heat capacities of the samples of both chips are not equal, i.e. the same perturbations in the reference temperature of the thermopiles produce different noise signals. On the other hand, there is a correlation between the outputs of the thermopiles. Therefore, it should be possible to create a dynamic model in order to convert the signal of the reference chip into a suitable correction signal. For the experimental identification of the model, a stochastic perturbation of the control temperature of the inner thermostat was generated. Fig. 5a shows the response of both thermopiles to the perturbations. Using these signals the parameters of a simple ARX model [13] were estimated by help of the system identification toolbox of MATLAB (MathWorks Inc., USA). The model as presented by Eq. (1) is a time-discrete simulation of the transfer function of a linear system with the thermopile voltage signals U_r (reference chip) and U_m (measuring chip) as input and output, respectively. It is the simplest version of a parametric black-box model. During the normal operation of the system U_r is measured in parallel with U_m . The processing of the calculation signal as well as the correction of the measurement signal can be performed in real-time or off-line (Fig. 6). As shown in Fig. 5b temperature induced disturbances can be suppressed by factor 10. The signals in Fig. 5b were also generated by stochastic perturbations of the control temperature of the thermostat.

$$U_m(t) + a_1 U_m(t - T_0) + \dots + a_4 U_m(t - 4T_0) = b_1 U_r(t - T_0) + \dots + b_4 U_r(t - 4T_0) \quad (1)$$

where T_0 is the sampling time.

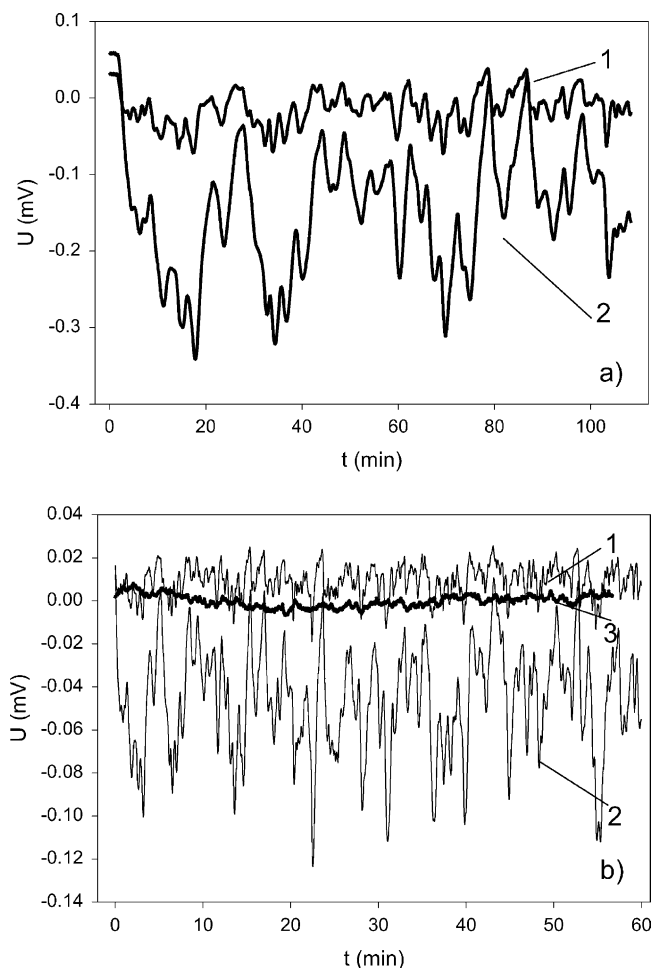


Fig. 5. Signal correction: (a) signals measured during the identification run (1, 2—thermopile voltage of the reference and measuring chip, respectively); (b) measured and corrected signals from the application run (1, 2—thermopile voltage of the reference and measuring chip, respectively, 3—corrected measuring signal).

3.2. Performance of the signals

In Fig. 7 the course of the temperature at selected positions of the system is shown. The periodic fluctuations of the room temperature (T_s in Fig. 7a) measured near the peltier module are caused by the air condition system of the laboratory. The temperature deviations of the controlled walls of the outer and inner frame are 40 and 5 μK , respectively (not included in the figure). The stability of the temperature

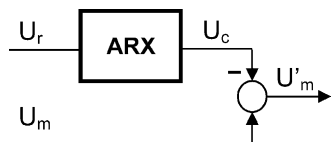


Fig. 6. Correction scheme (U_r , U_m —measured thermopile voltage of the reference and measuring chip, respectively; U_c —calculated correction signal; U'_m —corrected measuring signal; ARX—time-discrete dynamic model determined during the identification run).

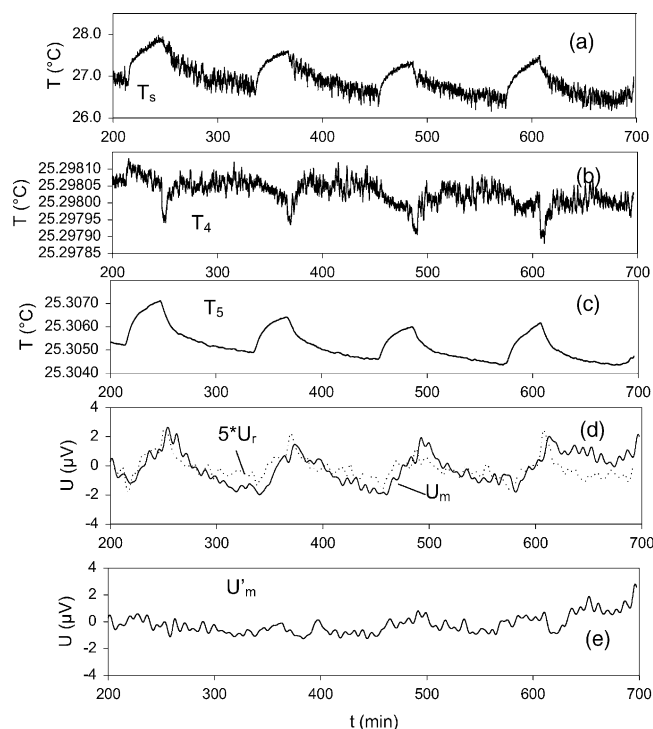


Fig. 7. Comparison of temperatures and signals in the system (T_s —surrounding temperature; T_4 —measuring thermistor located inside the wall of the inner frame; T_5 —thermistor located at the measuring chip (see Fig. 1); U_r , U_m —thermopile voltage of reference and measuring chip, respectively; U'_m —corrected measuring signal).

measurement is 4.3 μK , which was proved by substituting one of the thermistors by a precision resistor. The temperature of the non-controlled wall of the inner frame responds to the room temperature change by deviations of 100 μK (T_4 , Fig. 7b). The temperature changes at the upper chip exceed 1 mK (T_5 , Fig. 7c). Obviously, the chip arrangement is not perfectly enough coupled to the walls. This causes disturbances in the thermopile voltage of a few microvolts as shown in Fig. 7d. Applying the correction procedure as described above the base line deviations can be reduced to a level of $\pm 0.4 \mu\text{V}$ which corresponds to 180 nW (Fig. 7e). The low level of the reference signal requires a strong noise reduction before calculation of the correction signal.

To demonstrate the signal resolution of the system a low heat power reaction was measured. In Fig. 8 the calorimetric signal for the TRIS protonisation using a 0.5 mmol l^{-1} hydrochloric acid solution is plotted. The measurement was performed in continuous flow mode. A signal resolution in the nano-watt range seems really possible.

3.3. Enzyme catalysed oxidation of glucose

The plots in Fig. 9 are to demonstrate the applicability of the chip calorimeter to typical biochemical processes. In each case, a signal in the continuous flow mode and the impulse injection mode is shown. Fig. 9a depicts one period of a sequence of consecutive reaction steps performed in

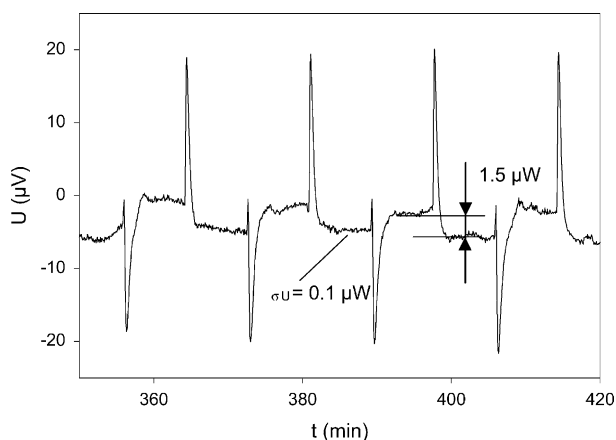


Fig. 8. Corrected measuring signal from TRIS protonisation reaction ($v = 15 \mu\text{l min}^{-1}$, $c_{\text{TRIS}} = 0.1 \text{ mol l}^{-1}$, $c_{\text{HCl}} = 5 \times 10^{-4} \text{ mol l}^{-1}$, $\sigma_U =$ standard deviation of the signal in steady-state).

the continuous flow mode. The heat power pulse shown in Fig. 9b is after subtracting of the pressure effects. In Fig. 9c the dependence of the steady-state voltage on the volume flow rate is presented. Obviously an optimal flow rate exists which is determined by the rate of reaction, the flow

rate dependent sensitivity and the degree of mixing. The results are also presented in order to emphasise the effect of the pumping mode on the mixing behaviour. Two series of measurements were done, using the syringe pump and the piezo-membrane micro-pump XXS500, respectively. The injection of the liquid by the syringe pump is almost continuously. The pulse volume of the used micro-pump is approximately $0.4 \mu\text{l}$ corresponding to a pulse frequency of less than 1 Hz. Probably the strong fluid pulses generate additionally mixing effects which lead to larger calorimetric signals. In Fig. 9d the heat effects of the injection of $10 \mu\text{l}$ volume increments are shown dependent on the concentration of the glucose solution. The saturation of the signal near 1 mmol l^{-1} is determined by the concentration of the solved oxygen (0.24 mmol l^{-1}).

3.4. Degree of conversion

At the used volume flow rates the flow in the reaction chamber is laminar, i.e. mixing is achieved by molecular diffusion. For the optimisation of the construction of the reaction chamber as well as the operation conditions the knowledge of the achieved degree of mixing for a given reaction is desirable. From the literature some methods

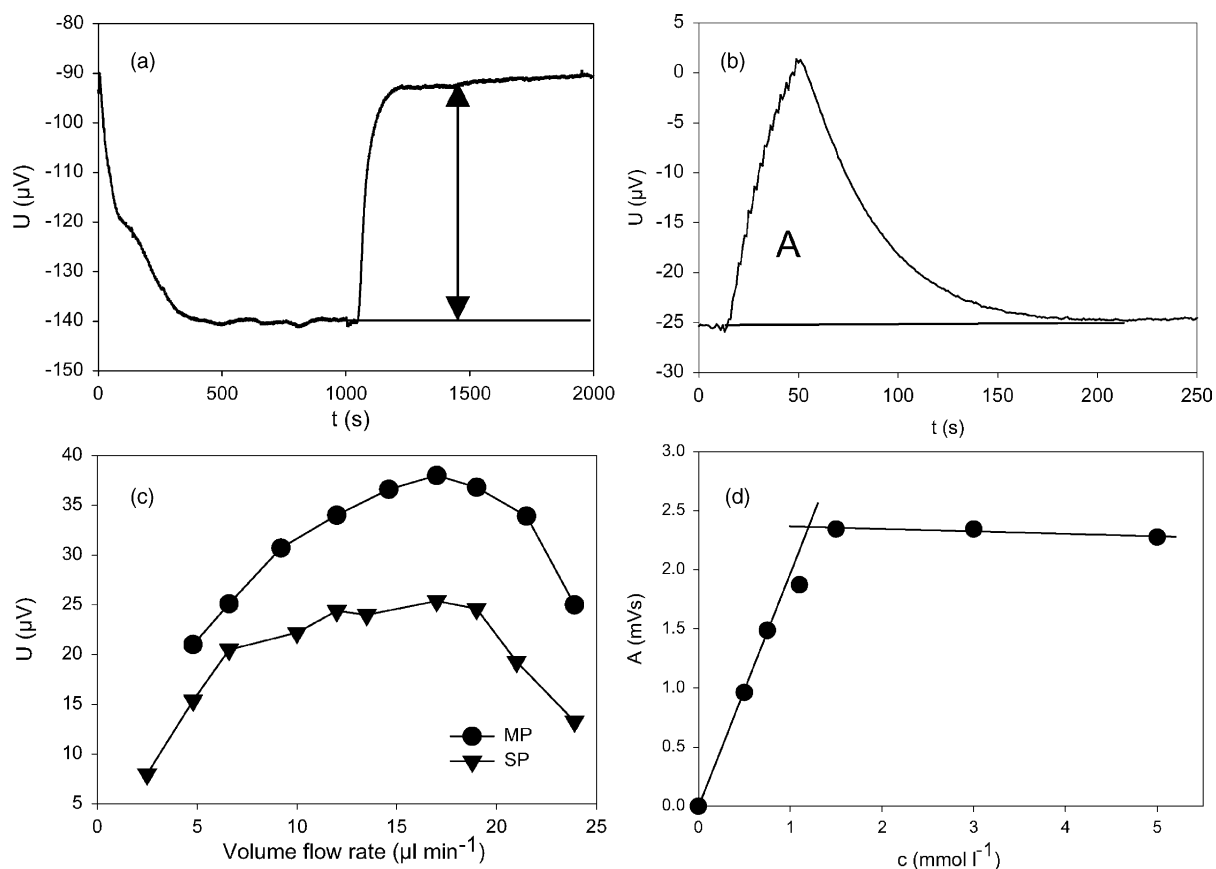


Fig. 9. Application of the enzyme catalysed glucose oxidation: (a) steady-state signal U_s from continuous flow mode operation, $c_{\text{gluc}} = 1.1 \text{ mmol l}^{-1}$, $v = 16.7 \mu\text{l min}^{-1}$; (b) impulse injection of $7.5 \mu\text{l}$, $c_{\text{gluc}} = 5 \text{ mmol l}^{-1}$, $v = 10 \mu\text{l min}^{-1}$; (c) flow rate dependence of the steady-state signal for syringe pump (SP) and micro-pump (MP) application; (d) peak integrals A of impulse injections dependent on the glucose concentration, $V = 10 \mu\text{l}$, $v = 10 \mu\text{l min}^{-1}$.

are known which are using special test reactions (e.g. the formation of iron rhodanide [14], the iodide–iodate reaction system [15] or pH changes in buffer solutions [16]) to study the mixing efficiency of micro-reactors. Because the degree of mixing depends on the diffusion coefficients of the involved species the results of such studies are only relative ones. If the enthalpy of the studied process is known then the calorimetric signal can be used to calculate the degree of mixing. In Eq. (2) the degree of mixing D_{mix} is calculated from the measured steady-state voltage U_s , the sensitivity S and the maximum heat power p_{max} . The latter is determined by the enthalpy, the volume flow rate and the concentration of the substrate. Unfortunately, it is difficult to obtain accurate data for the sensitivity of micro-sized calorimeters [11,17]. To avoid this problem, we have developed a new method for the determination of the degree of mixing based on the comparison of the amounts of converted and non-converted substrate during a stopped-flow measurement:

$$D_{\text{mix}} = \frac{U_s}{Sp_{\text{max}}} \quad (2)$$

$$t_r = \frac{V_{\text{ch}}}{v} \quad (3)$$

$$n_c = (c_i - c_o)v t_r \quad (4)$$

$$D_{\text{mix}} = \frac{n_c}{n_c + n_2 - n_1} \quad (5)$$

$$n_c = \frac{U_s}{S(v)} t_r \frac{1}{\Delta H} \quad (6)$$

$$n_2 - n_1 = \frac{1}{S(v)} (A_2 f_s - A_1) \frac{1}{\Delta H} \quad (7)$$

$$f_s = \frac{S(v)}{S(v=0)} \quad (8)$$

$$D_{\text{mix}} = \frac{U_s t_r}{U_s t_r + f_s A_2 - A_1} \quad (9)$$

where ΔH is the reaction enthalpy.

Fig. 10a depicts schematically the distribution of the concentration of the substrate inside the reaction chamber. For simplification linear geometry is assumed. The shown distribution is presumed to be valid in steady-state. The fluid enters the reaction chamber with the substrate concentration c_i and leaves it with concentration c_o . The non-converted substrate which is accumulated inside the reaction chamber is equal the integral of the concentration over the chamber volume V_{ch} . After the fluid flow is stopped the reaction continues until complete conversion of the accumulated substrate (n_2 in Fig. 10b). The totally accumulated amount n_2 consists of two parts. The amount n_1 which corresponds to the area above the dashed line in Fig. 10a is accumulated during the transition phase. The area below it corresponds to the non-converted part of the substrate which is injected in steady-state with the

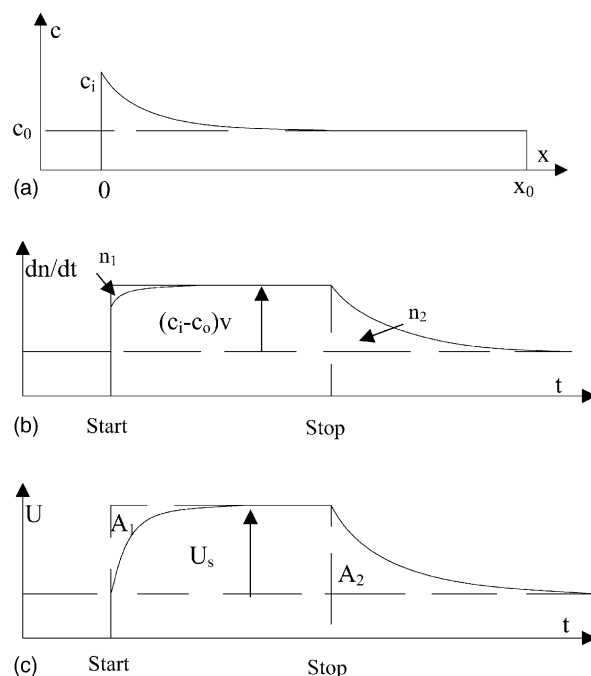


Fig. 10. Degree of mixing from calorimetric stopped-flow measurement: (a) concentration distribution of the substrate inside the reaction chamber (c_i , c_o —input and output concentration, respectively; x —linear dimension of the reaction chamber, x_0 —outlet position); (b) schematic course of the rate of conversion during a stopped-flow experiment (n_1 —amount substrate accumulated during transition phase, n_2 —amount of substrate which reacts after stop of fluid flow, v —volume flow rate); (c) schematic signal of a stopped-flow measurement (U_s —steady-state voltage during flow phase, A_1 , A_2 —areas which have to be determined).

volume flow rate v during the residence time t_r (Eq. (3)). The amount of substrate n_c which is converted during the same time results from the difference of the input and output concentration (Eq. (4), Fig. 10b). Assuming a fast reaction the degree of mixing can be expressed according Eq. (5). By help of Eqs. (6)–(9) the degree of mixing can be calculated using the parameters of the calorimetric signals (Fig. 10c). Further, the relation of the sensitivity at volume flow rate v and $v = 0$ has to be known ($S(v)$ and $S(v = 0)$, respectively), i.e. the calculation is not completely independent of the sensitivity. But in comparison with Eq. (2) errors in the sensitivity have a much smaller effect.

Using Eq. (9) we have calculated the degree of mixing for both test reactions at different volume flow rates. Up to $30 \mu\text{l min}^{-1}$ complete mixing was found in the case of the TRIS protonisation. The enzyme catalysed oxidation of glucose is a slow reaction regarding the present residence time. Therefore, Eq. (9) provides the degree of conversion including both mixing and kinetic effects. For the series of measurements performed with the syringe pump the degree of conversion is approximately 0.7. The larger signals for the micro-pump-based measurements can be really explained by an improved mixing efficiency. The degree of conversion is increased to values higher than 0.8.

4. Conclusion

The application of chip calorimeters for solving biochemical problems requires a heat power resolution near the physical determined limits. A heat power detection limit lower than 50 nW is prevented by the large electrical resistance of integrated thermopiles because of thermal and amplifier noise. Further, larger time constants accompanied with the use of liquid samples increase the necessary effort for temperature control. However, differential chip arrangements and temperature control with a precision better than 100 μ K enable the monitoring of heat power evolution in the nano-watt range. This opens the way for relevant applications in bio-solution chemistry.

Acknowledgements

Financial support of German Research Council (Deutsche Forschungsgemeinschaft, Wo576/5-3) and AiF (BMWA, AiF-Nr. 13328 BR/1) is gratefully acknowledged.

References

- [1] A.W. Van Herwaarden, P.M. Sarro, Thermal sensors based on the Seebeck effect, *Sens. Actuators* 10 (1986) 321–346.
- [2] J.M. Koehler, M. Zieren, Chip reactor for microfluid calorimetry, *Thermochim. Acta* 310 (1–2) (1998) 25–35.
- [3] J. Lerchner, A. Wolf, G. Wolf, Recent developments in integrated circuit calorimetry, *J. Therm. Anal. Calorim.* 57 (1) (1999) 241–251.
- [4] J. Lerchner, A. Wolf, A. Weber, R. Huettl, G. Wolf, J.M. Kohler, M. Zieren, On-line monitoring of enzyme activities using microreactor heat power meters, in: *Microreaction Technology: Industrial Prospects*, Proceedings of the Third International Conference on Microreaction Technology, Frankfurt, April 18–21, 1999, p. 1999.
- [5] A. Wolf, A. Weber, R. Huettl, J. Lerchner, G. Wolf, Sequential flow injection analysis of complex systems using calorimetric detection, *Thermochim. Acta* 382 (1–2) (2002) 89–98.
- [6] Xensor Integration, Delft, NL. <http://www.xensor.nl>.
- [7] J. Lerchner, R. Kirchner, J. Seidel, D. Waehlich, G. Wolf, Determination of molar heats of absorption of enantiomers into thin chiral coatings by combined IC calorimetric and microgravimetric (QMB) measurements. I. IC calorimetric measurements of heats of absorption, *Thermochim. Acta*, in press.
- [8] D. Caspary, M. Schroeffer, J. Lerchner, G. Wolf, A high resolution IC-calorimeter for the determination of heats of absorption onto thin coatings, *Thermochim. Acta* 337 (1–2) (1999).
- [9] S.A. Adamovsky, A.A. Minakov, C. Schick, Scanning microcalorimetry at high cooling rate, *Thermochim. Acta* 403 (1) (2003) 55–63.
- [10] S.L. Lai, G. Ramanath, L.H. Allen, P. Infante, Z. Ma, High-speed scanning microcalorimetry with monolayer sensitivity, *Appl. Phys. Lett.* 67 (9) (1995) 1229–1231.
- [11] C. Auguet, J. Lerchner, V. Torra, G. Wolf, Identification of micro-scale calorimetric devices, *J. Therm. Anal. Calorim.* 71 (2) (2003) 407–419.
- [12] J. Lerchner, G. Wolf, A. Torralba, V. Torra, Ambient perturbation reduction in micro-sized calorimetric systems, *Thermochim. Acta* 302 (12) (1997) 201–210.
- [13] L. Ljung, *System Identification: Theory for the User*, Prentice-Hall, Englewood Cliffs, NJ, 1987.
- [14] W. Ehrfeld, K. Golbig, V. Hessel, H. Loewe, T. Richter, Characterization of mixing in micromixers by a test reaction: single mixing units and mixer arrays, *Ind. Eng. Chem. Res.* 38 (1999) 1075–1082.
- [15] P. Guichardon, L. Falk, Characterization of micromixing efficiency by the iodide–iodate reaction system. Part I. Experimental procedure, *Chem. Eng. Sci.* 55 (2000) 4233–4243.
- [16] L.D. Scampavia, G. Blankenstein, J. Ruzicka, G.D. Christian, A coaxial jet mixer for rapid kinetic analysis in flow injection and flow injection cytometry, *Anal. Chem.* 67 (1995) 2743–2749.
- [17] J. Lerchner, G. Wolf, C. Auguet, V. Torra, Accuracy in integrated circuit (IC) calorimeters, *Thermochim. Acta* 382 (1–2) (2002) 65–76.